

## Synchronized System for Wireless Sensing, RFID, Data Aggregation, & Remote Reporting

Steven W. Arms\*, Christopher P. Townsend, Jacob H. Galbreath, David L. Churchill, Nam Phan^

\* President  
MicroStrain, Inc.  
Williston, Vermont  
[swarms@microstrain.com](mailto:swarms@microstrain.com)

^ Division Head (Acting) Structures  
U.S. Navy/NAVAIR  
Lexington Park, Maryland  
[nam.phan@navy.mil](mailto:nam.phan@navy.mil)

### ABSTRACT

We report on the development and test of an integrated structural health monitoring and reporting (SHMR) system for use on Navy aircraft. Our goal was to develop and test a versatile, fully programmable SHMR system, designed to synchronize and record data from a range of wireless and hard wired sensor and active RFID networks. Wireless sensors include strain gauges, accelerometers, and load/torque cells. Data were collected at multiple sampling rates and time stamped and aggregated within a single scalable database on a base station, termed the wireless sensor data aggregator (WSDA). The WSDA, in addition to providing a central location for collecting data, also provided a beaconing capability to synchronize each sensor node's embedded precision timekeeper. High speed wireless sensor nodes were demonstrated to be capable of logging data at sample rates of up to 50 K samples/second, while consuming ~9 milliamps at 3 VDC (27 milliwatts). The high sample rate nodes can operate perpetually, without batteries, by using miniature vibration energy harvesters, which provided 37 milliwatts of continuous DC power under conditions replicating a helicopter gearbox. Scalable networks of RFID nodes with > 20 years coin cell battery life were also demonstrated. Wireless node network initial synchronization in response to a centrally broadcast network command, such as to initiate node sampling, or to synchronize node time keepers, was measured at +/- 4 microseconds. With the time synchronization beacon sent only at the onset of a two hour long test, and with simultaneous exposure to temperatures of -40 to +85 deg C, the system's timing accuracy was ~5 milliseconds. The system was demonstrated to be capable of supporting both high sample rate burst and periodic sampling modes, with accurate wireless network timing synchronization.

### INTRODUCTION

Direct loads tracking of helicopter rotating components, combined with active radio frequency identification (RFID) has the potential to reduce maintenance costs, reduce weight, maximize structural life, & enhance safety. As the fleet ages, there is an increasing need for embedded wireless sensors capable of detecting and tracking accumulated damage. Maley et al of the US Navy emphasized the need for embedded, wireless sensors capable of detecting and tracking the "precursors" to crack initiation<sup>1</sup>. The overarching vision is to deploy distributed, autonomous wireless sensor networks along with RFIDs and bar codes to provide a wealth of usage information about an entire aircraft to enable next generation structural health monitoring<sup>2,3</sup>. In order for these structural health monitoring (SHM) systems to be accurate, it is critical that the data from various wireless and hard wired sensors be accurately time stamped.

We previously reported on energy harvesting, wireless sensor modules which were integrated into the pitch link of a Bell M412 helicopter, and successfully flight tested<sup>4,5</sup>. Pitch link loads were recorded & periodically transmitted into the cabin, demonstrating that an energy harvesting direct loads tracking sensor can operate continually without battery

maintenance. By combining structural load tracking with a network of RFIDs, a rich amount of information can be collected and used to optimize aircraft maintenance.

### OBJECTIVES

Our main objective in advancing this technology has been to develop a system that can automatically synchronize, aggregate, & report data from a network of wireless sensors and RFIDs. Design criteria for our active RFID tags include small size, long battery life, fast read times, and local data storage capacity. Requirements for the wireless sensor data aggregator (WSDA) included support for both wireless and hard-wired sensors, the global positioning system (GPS), and the vehicle bus, all with an open architecture interface. Below we provide our four (4) main objectives:

1. Develop and test a wireless data aggregator (WSDA), capable of synchronizing wireless & hard-wired sensor networks, aggregating these data, and providing an open architecture communications interface to existing health and usage monitoring systems (HUMS).
2. Document the accuracy of wireless sensor network time synchronization.
3. Develop and test a high sample rate wireless sensor node capable of data acquisition at programmable rates up to ~50 K samples/second and capable of operating solely from

---

Presented at the American Helicopter Society 65th Annual Forum, Grapevine, Texas, May 27-29, 2009. Copyright © 2009 by the American Helicopter Society International, Inc. All rights reserved.

the energy provided by a miniature vibration energy harvester mounted on a helicopter gearbox.

4. Demonstrate system compatibility with a scalable network of active RFIDs, suitable for use on military aircraft.



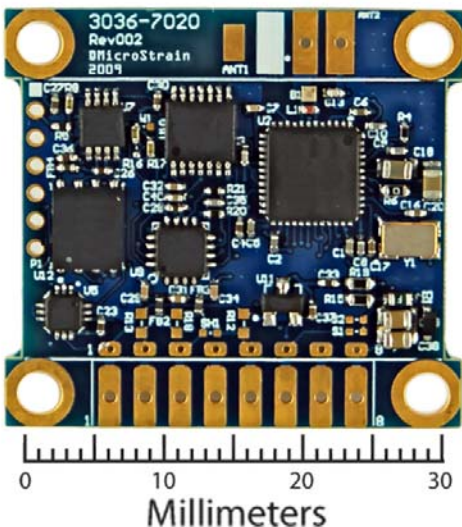
**Figure 1. Wireless Sensor Data Aggregator (WSDA) collects time-stamped data from wireless/wired sensors.**

## METHODS

### High Sample Rate Wireless Sensor Node

A high sample rate (HSR) node was designed by MicroStrain, Inc. to log data at 50 kilosamples per second (kSPS) with 12-bit ADC resolution. The HSR node can be configured to sample a full differential Wheatstone bridge input (strain gauges, accelerometers, pressure sensors, etc.) or a single-ended 0-3 volt input. Each high rate logging event may consist of 125K samples, or ~2.25 seconds of record time when sampled at 50 kSPS. The node can store up to 1 million samples on its embedded, non-volatile memory chip (Figure 2).

**Figure 2. High sample rate (50 K samples/sec) wireless sensor node.**



The HSR node measures only 31x31x5 mm including mounting tabs and operates from a 3 volt DC supply. When logging data continuously at 50 kSPS, average current consumption was measured at 8.8 mA (26.4 mW). When actively transmitting digital data from non-volatile memory (along with framing and checksum bytes), the average current consumption was 25 mA (75 mW). When in sleep mode, current consumption was only 20 microamperes (.060 mW). To test performance, a signal generator was used to produce a 1 kHz sine wave input (reference) signal, and this reference waveform was sampled using the HSR node's single ended input.

### Vibration Energy Harvester

The energy harvester was excited by vibrations that reproduced those measured from a Helicopter Main Gear Box . A photograph of the prototype harvester is provided below in Figure 3.



**Figure 3. MicroStrain's vibration energy harvester shown adjacent to a US quarter dollar**

The harvester's output was collected in a capacitive energy storage circuit, and "consumed" by a fixed load resistor. The absolute and normalized power output values for the energy harvester are shown in Tables I and II. These data provide a guide to design of the harvester for a given high sample rate vibration monitoring application, given the power consumption specifications as provided in the previous section. For example, assuming a vibration harvester of 4.3 cubic centimeters (cc) and 38.5 grams is suitable for the application, we can expect this harvester to generate 37 milliwatts continuously when mounted on this particular Helicopter Gear Box.

The duty cycle of the sensing node can be adjusted, or the harvester can be re-sized, to meet the needs of the particular monitoring application. The output of our vibration harvesters increases approximately linearly with both mass and volume. The power consumed by the sensing node decreases significantly as the interval between samples is increased. The calculated average power consumption of our wireless nodes for a range of sample intervals are provided in the next section.

**Table I. Absolute Energy Harvester Power Output, Helicopter Main Gear Box.**

Load Resistor (Ohms)	Rectified Output Voltage (VDC)	Power Output (mW)
600	4.7	37

**Table II. Normalized Energy Harvester Power Output, Helicopter Main Gear Box.**

Mass (grams)	Volume (cc)	Power Density (mW/cc)	Specific Power (mW/kg)
38.50	4.30	8.60	961

**High Sample Rate Energy Consumption w/ Duty Cycling**

The high sample rate node, as well as the other nodes in the network, will support scheduled data logging according to programmable time intervals (duty cycles), along with periodic RF transmission. Shorter duration sampling duty cycles will result in longer sleep durations, as well as reduced "on" time for radio transmissions. Therefore, periodic time interval sampling or "duty cycling" can greatly reduce the average power consumption, as we illustrate in the following example.

In this example, 50 kSPS data are collected for a relatively short (1 second) duration, or "burst", at a time interval of once per minute (60 seconds). The time duration required for wireless data transmission can be calculated by dividing the number of samples recorded by the wireless data transmission rate. Digital wireless data transmission, using an efficient 802.15.4 protocol with framing and error checking, can be accomplished at a rate of 4000 SPS. This information, along with power consumption for various operational modes, allows the average power consumption to be calculated by the following expression:

Average power consumed = (data logging duty cycle)\*(power consumed when logging) + (wireless data transmission duty cycle)\*(power consumed when transmitting) + (sleep duty cycle)\*(power consumed when sleeping).

Where the power consumed when logging = 26.4 mW; transmitting = 75.0 mW; and when sleeping = .060 mW. And where the data logging duty cycle= 1sec/60sec = 1.67%; the wireless data transmission duty cycle = 12.5sec/60sec = 20.83%; and the sleep duty cycle = 77.5%.

Therefore, the average power consumed = 1.67%\*26.4+ 20.83%\*75 mW + 77.5%\*.060 mW = **16.1 mW**. This power consumption is ~44% of the gearbox vibration harvester's output (37 mW). Therefore, sampling at 50 kSPS rates for 1 second every minute can be perpetually sustained, without batteries, in the gearbox application.

Our system was designed to be fully programmable, and therefore, fully adaptable to the needs of specific vibration monitoring applications. In Table III below, we provide the average power consumption (in mW) for 50 kSPS data collected for 0.1 sec, 0.5 sec, and 1 second durations at time intervals of once per minute, once per 10 minutes, once per hour, and once per day. Longer time intervals between data acquisition bursts would allow smaller, lower mass energy harvesters to sustain operation.

**Table III. Average power consumption (mW) for 50 kHz data acquisition at various time intervals & durations**

Sample duration (sec)	Acquisition Interval			
	1 min	10 min	1 hour	1 day
0.1	1.67	0.22	0.09	0.06
0.5	8.09	0.86	0.19	0.07
1.0	16.1	1.66	0.33	0.07

**Data Aggregation**

The wireless sensor data aggregator (WSDA, Figure 1) is responsible for time synchronized data collection from wireless and hard wired networks. Important design criteria for the WSDA were:

- Open architecture operating system
- Provides time synchronization platform
- Data saved in scalable sensor database, supporting flexible data types, sample rates, data base queries, and sorts
- Multiple bus interfaces supported:
  - IEEE802.15.4
  - Ethernet (HUMS)
  - RS232/RS422 (HUMS)
  - USB
  - 1553B aircraft bus
  - CAN

**Data Synchronization**

One of the challenges for a distributed multi-network topology is synchronizing all the data acquisition nodes throughout the entire system. Figure 4 provides a block diagram of the WSDA and associated hard-wired and wireless nodes. WSDA functional blocks include the GPS receiver, timing engine, microprocessor (uP) core running Linux 2.6, CAN bus controller, and wireless controller.

The data aggregator and wireless sensor nodes feature a precision, nanopower, temperature compensated timing engine, or real time clock (RTC) which uses an onboard temperature sensor, calibrated look-up tables, and an oscillator tuning mechanism to maintain a highly accurate frequency of +/- 3 parts per million (PPM) over an operating temperature range of -40 to +85 deg C.

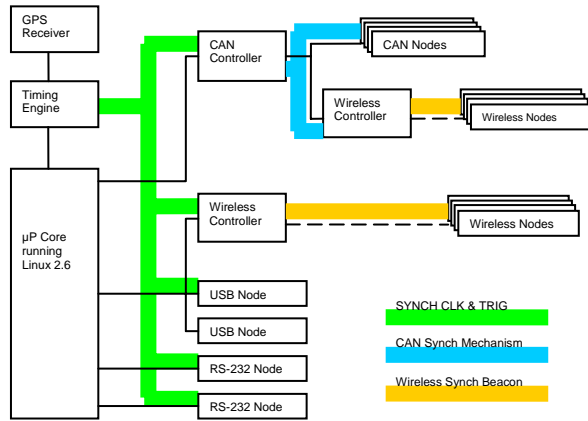


**Figure 4. Wired/Wireless Sensor Nodes and WSDA System Functional Block Diagram.**

The real time clocks on all wireless and wired sensor nodes are synchronized at the beginning of a test to the base station’s time reference, using a wireless beacon to communicate that reference. The WSDA base station uses a Global Positioning System (GPS) 1 pulse per second (PPS) clock as the default timing reference. In the event that GPS is not available, the WSDA switches to its internal +/- 3 PPM real time clock as the timing reference to insure synchronization of all the remote sensor nodes to the WSDA’s clock. With either timing source, the WSDA’s timing engine provides a stable 1 Hz reference for the transmitted synchronization beacon. On the wireless sensor nodes, the same timing engine is slightly modified to provide adjustable output from 1 Hz to 4096 Hz, which is used to drive a sensor-sampling interrupt on the host processor.

Precise timing enables the aggregated data from the network to be accurately time stamped, but it also enables scaling of the wireless network. Combining time division multiple access (TDMA), carrier sense multiple access (CSMA), and frequency division multiple access (FDMA), the synchronized network can support a large number of wireless sensor nodes. The system’s aggregate sensor sampling rate with continuous digital wireless communications may be estimated at ~10,000 samples/sec per radio channel (at up to 16-bit sensor data resolution). For example, assuming a network of wireless strain nodes were configured to sample a 3-axis strain gauge rosette at a rate of 33 samples per second, this system will support up to 100 distinct wireless nodes (300 strain gauges) using only TDMA and CSMA techniques on a single radio communication channel. By adding radio transceiver chips, or by scanning radio channels within the WSDA base station, the system will theoretically support 16 of these strain sensing networks, or as many as 300 strain gauges\*16 radio channels = 4,800 individual strain gauges.

### Application Programming Interface

To support external systems, such as HUMS boxes, an open architecture application programming interface (API) for our wireless sensor data aggregator has been authored. The API is implemented as a web service using standard http request commands. Using the web service model keeps the API Interface open and easily adapted to many platforms. The response for each command is an xml document that contains the status of the command. Each command returns a response in the form of an xml document. XML was used as the response because it is a platform independent interchange format that is widely supported. A few examples of the API commands are provided below:

- *StartSession* command is called to begin a data logging session with the nodes. When the command is called, the WSDA synchronizes all wired and wireless nodes using the beacon, then goes into collection mode and records data from all nodes in the database.
- *StopSession* command is called to end a data logging session.
- *ResetDatabase* command will clear all the data currently stored in the database.
- *NodeInfo* command is called to retrieve a list of all the nodes and associated information currently stored in the database.
- *Download* command is called to retrieve a range of data for a single node from the database.

### Remote Reporting

To enable report data reporting, the WSDA includes an internal cellular modem and, will, in the future, support an external satellite modem. The remote cellular GSM/GPRS interface uses HTTPS and SSH protocols for secure transfer of data to a remote server. We selected a cellular modem based on a trade study, and chose the GSM/GPRS modem because it offered the widest global cellular coverage. We have begun integration of a micro-miniature satellite transceiver with our system that utilizes the Globalstar satellite network. This network provides a good combination of worldwide coverage at a reasonable cost per byte of data transferred.

Data sets stored on the WSDA were transferred to a web server for development, test, and demonstration purposes. A flash & HTML web interface was created to enable ongoing, completely independent structural monitoring. A dedicated hosting entity was selected to provide a scalable, reliable, and secure dedicated server. In order to provide secure access to the data stored on our remote server, a password protected user management and authentication process was implemented.

### Time Synchronization Accuracy Testing

To characterize this single packet communication latency, a digital oscilloscope was used to measure the time between the completion of packet transmission on the wireless network controller, and completion of packet reception on the wireless sensor node. Due to the relatively short (<70 m) communication range of the 802.15.4 radio, it is assumed that differences in the propagation delay are negligible (<300 ns) and therefore ignored. Packet reception and decoding is handled by a hardware state machine in radio chip, with a measured radio reception jitter of ~400 ns. However, the total system jitter may be greater due to software handling of the received packet.

To measure the total system jitter, a series of tests were performed using MicroStrain's USB base station, four (4) MicroStrain SG-Link wireless strain nodes, a Tektronix 100 MHz 4-ch oscilloscope node with a separation distance of 2 meters between the wireless nodes and the USB base station (network controller). A broadcast command to initiate data logging was sent to the wireless (star) network of SG-Link nodes. Scope probes connected to the digital I/O lines corresponding to start of sampling for each of the four wireless node's A/D converters provided four digital signals corresponding to the initiation of the broadcast command. Tests were repeated 250 times to bound the minimum and maximum latency result.

To determine the relative timing drift of the wireless sensor node's time keepers with beacon synchronization at the start of the test only, two independent wireless strain sensing nodes (SG-LINKs, MicroStrain, Inc.) with integral precision timekeepers were used. In each of these tests, the timing beacon was sent only once – at the start of the test. Each SG-LINK node was provided with a common analog input voltage, provided by a rack-mounted laboratory function generator (B&K Precision, model 4011A). A saw-tooth waveform of 10 Hz frequency and 2.8 volts magnitude from the function generator was used as direct input to each of the SG-LINK nodes. This type of waveform was selected because the inflection point (peak) of a saw-tooth waveform may be identified even in the case that the data recorded by the sensor nodes were to miss the precise instant that the peak occurred. The wireless strain sensor nodes were configured to sample at a rate of 128 Hz, with timing sourced from the embedded temperature-compensated timing engine.

The wireless SG-LINK nodes were both placed in a temperature controlled environmental chamber, with the node electronics exposed to open air within the chamber, and no thermal insulation of any form. Each test was run while thermally cycling the nodes between -40° and +85° C at a ramp rate of 12.5° C per minute, for 2 hours duration, which provided ~6 complete thermal cycles. The WSDA collected the sensor data, which was later downloaded and plotted for analysis.

### Active RFIDs

Department of Defense (DoD) RFID Policy (<http://www.dodrfid.org>) identifies the following characteristics for active RFID tags: powered by an internal battery, capable of both read and write – enabling data in non-volatile tag memory to be rewritten or modified. Read-write capability is an important feature, as it allows structural tags to include critical data such as the time and date of specific flights on a specific aircraft, the number of flight hours, the lifespan expended (for fatigue sensitive components), and the estimated remaining life (assuming continued use at the present estimated fatigue rate). Alternatively, a database can be maintained on a remote server which relates specific RFIDs to a particular aircraft's usage histories. The advantage of storing data on the tag itself is that the part's history may be viewed without requiring access to a remote database.

A micropower RFID module was designed, built and tested (Figure 5). This module utilized a very small coin cell battery and features embedded protocols to extend battery life by leveraging the processor's inherent micropower sleep modes. The nodes feature an integral surface mount chip antenna, which was demonstrated to work well even when the node is placed on a metal surface. A sealed package has been developed and has been demonstrated to protect the module during operational tests, performed to MIL-STD-810F over temperatures of -40 to +85 deg C, and over extremes of humidity, vibration, and inertial shock. The nodes feature 512 kbytes non-volatile memory.



**Figure 5. MicroStrain active RFID module, unpackaged, w/ battery & antenna, adjacent to US quarter.**

The RFID node's embedded firmware supports two modes of operation. The first mode is an autonomous, periodic transmit-on-schedule (ToS) protocol of RFID data. The second mode uses an autonomous, periodic transmit-on-demand (ToD) protocol. In ToD mode, the RFIDs transmit their packet only upon receipt of an encoded over-the-air request from the WSDA (or any other reader running the proper protocols). The transmitted data packet includes the DoD 96 bit RFID, framing bytes, and checksum bytes. The DoD 96 bit code includes a serial number and enables unique IDs for up to  $2^{96} = 7.9 \times 10^{28}$  tagged items.

The data aggregator identifies each individual node's 96 bit electronic product (EPC) code, and checks the received packet against the checksum to insure the entire data packet was received reliably. The update rates for ToS and ToD modes are fully programmable and embedded within non-volatile memory.

Testing was performed to determine the active RFID node's average power consumption for both modes of operation and at various update rates. These results are provided in the section that follows. We also provide an analysis of the scalability of the active RFID network given the node's pre-programmed rates.

## RESULTS

### High Sample Rate (HSR) Node Sampling Fidelity

Tests using a reference 1 KHz sinusoidal waveform produced the data provided below in Figure 6. These data plot the reference signal as recorded by a digital oscilloscope (Tektronix model TDS 2014) along with the data recorded by the HSR node. The strong match of these two data sets confirms the basic performance of the HSR node. More exhaustive testing is ongoing, and will be included in future publications.

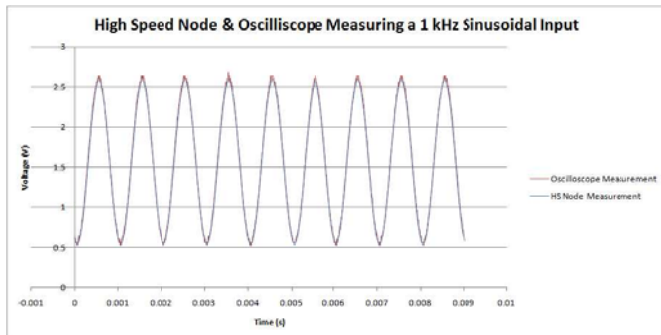


Figure 6. Sample 1 kHz data set collected by HSR node at 50 kSPS rate and plotted along with scope trace

### Initial Synchronization Timing Performance

Recordings in response to a beaoned network broadcast address command are provided below in Figure 7. Tests were repeated 250 times, and all timing jitter was bound within a maximum envelope of  $\pm 4$  microseconds.

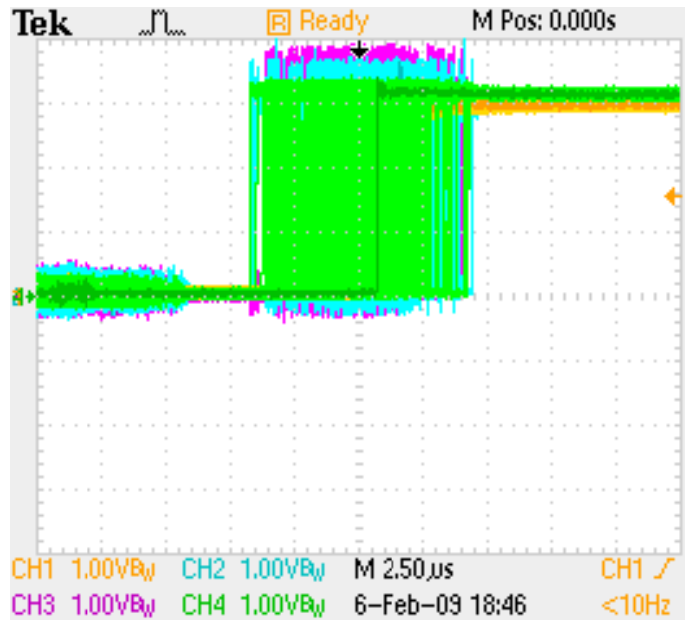


Figure 7. Scope traces indicating initial sample timing for four separate wireless nodes responding to a broadcast command. This test was repeated 250 times, and all timing jitter was bounded at  $\pm 4$  microseconds.

### Timing Accuracy

For the 2 hour timing test with beacon correction provided only at the start, and with the strain nodes cycled from  $-40$  to  $+85$  deg C, a timing offset of 5.71 milliseconds was measured between the two nodes, as shown in Figure 8. This constitutes a relative clock drift rate of 0.79 PPM. An additional 2 hour test was performed over the same temperature range using a lower frequency saw-tooth wave voltage input of 1Hz, in order to check our prior result. This additional short term test yielded a timing offset between the two SG-LINK nodes of 5.04 milliseconds, or 0.7 PPM, which agreed closely with our prior result.

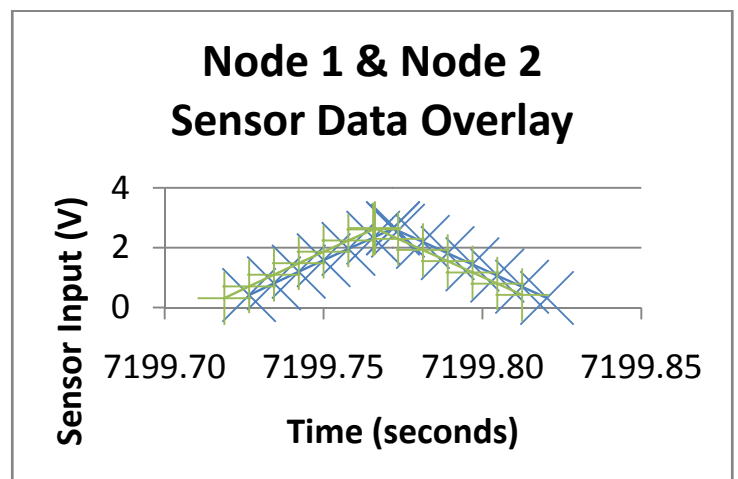


Figure 8. Timing synchronization w/ beacon sent once - at start of 2 hr exposure to  $-40$  to  $+85$  deg C: 5.7 millisecc.

## RFID Power Consumption & Battery Life

The lowest power consumption mode for active RFID nodes was measured for the transmit on demand (ToD) operational mode. Average RFID currents (at 3 VDC) were measured at 22 microamps for a 1 second listen/transmit rate, and 2.7 microamps for a 30 second listen/transmit (LT) update interval.

Battery life will depend on the battery's capacity and the programmed update interval. For a Tadiran (Port Washington, NY) coin cell of 550 mAh capacity (model TLH-2450, 24mm dia. x 6 mm thick), and with an L/T rate of 30 seconds, the battery would last for ~23 years. For applications that cannot support a primary battery, or when an extremely low profile is needed, a thin film lithium ion battery (Infinite power Solution, Golden, CO) may be used in concert with an energy harvesting element. Provided that the thin film battery can be background recharged to its full capacity (0.7 mAh), and with the active RFID programmed for a 30 second L/T interval, the active RFID node will operate for ~10 days before require recharging. We note that the energy harvesting element can utilize one or more means to refresh the battery, including harvesting energy from vibration, strain, thermal gradients, solar radiation, or electromagnetic radiation<sup>6,7</sup>.

Scalability of the active RFID network is improved with longer L/T intervals. With an L/T rate of five seconds, and using our existing IEEE 802.15.4 radio transceiver protocols, the maximum number of RFID nodes that can be supported within range (~70 meters) of the WSDA node may be calculated at ~4000. With a 30 second L/T interval, this theoretical maximum increases to ~25,000 nodes. Allowing for transmission "overhead", we propose 50% of the maximum be used, which enables support for ~12,000 nodes.

## CONCLUSIONS

The beaconing system achieved an initial synchronization of +/- 4 microseconds and a long term timing accuracy of ~5 milliseconds over 2 hours with exposure to extreme (-40 to +85 deg C) environments. The timing accuracy improves when the thermal environment is stable. The timing accuracy is also improved by sending the beacon more frequently. For flight tests that require a synchronization of sensor data to sub-millisecond accuracies, a conservative approach would be to provide a synchronization beacon every 5 minutes.

For those applications where the timing synchronization may not need to achieve sub-millisecond accuracies, all wireless sensor radio communications may be turned off completely during flight. The wireless nodes would then be used in data-logging mode only, which conserves power and eliminates all propagation of the 2.4 GHz radio signal from the nodes during flight. Time stamped data can be collected from the wireless nodes after the flight is completed.

The system supports a network of programmable, high sample rate (50 KHz) sensor nodes, active RFID tags, and provides an open architecture interface to allow HUMS boxes to benefit from the elimination of wires and the associated reduction in weight and complexity. The high sample rate nodes can operate perpetually, without batteries, from the vibrations inherent on a helicopter gearbox.

The system is capable of remote reporting using mobile phone networks, with satellite reporting currently under development. These capabilities, coupled with appropriate wireless security methods, will enable critical structural sensor data to be managed remotely, securely, and automatically.

## ACKNOWLEDGMENTS

The authors thank the US Navy/NAVAIR for support under the DoD Phase II SBIR and ONR BAA programs. The US Navy does not endorse or recommend any particular product or process by supporting this project's R&D efforts.

## REFERENCES

- <sup>1</sup> Maley, S., Plets, J., Phan, N., "US Navy Roadmap to Structural Health and Usage Monitoring – The Present and Future", *American Helicopter Society 63<sup>rd</sup> Annual Forum*, Virginia Beach, VA, May 1-3, 2007
- <sup>2</sup> Sautter, F.C., Durant, R.W., "A CBM Environment as Enabled through the DoD Policies for Serialized Item Management (SIM) and Item Unique Identification (IUID)", *American Helicopter Society 64<sup>th</sup> Annual Forum*, Montreal, Canada, April 29 - May 1, 2008
- <sup>3</sup> Augustin, M., Yearly, D., Advanced Technologies for Rotor System Condition-Based Maintenance (CBM), *American Helicopter Society 64<sup>th</sup> Annual Forum*, Montreal, Canada, April 29 - May 1, 2008
- <sup>4</sup> Arms, S.W., Townsend, C.P., Churchill, D.L., Moon, S.M., Phan, N., "Energy Harvesting Wireless Sensors for Helicopter Damage Tracking", *American Helicopter Society Forum 62*, Health & Usage Monitoring Systems (HUMS), Phoenix, AZ, May 9-11, 2006
- <sup>5</sup> Arms S.W., Townsend, C.P., Churchill, D.L., Augustin, M., Yearly, D., Darden, P., Phan, N., "Tracking Pitch Link Dynamic Loads with Energy Harvesting Wireless Sensors", *American Helicopter Society Forum 63*, Virginia Beach, VA, May 2007
- <sup>6</sup> Churchill, D. L. Hamel, M. J. Townsend, C. P. Arms, S. W.: "Power Management for Energy Harvesting Wireless Sensors" *Proc. SPIE's Symposium on Smart Structures and Materials 2003: Smart Electronics, MEMS, BioMEMS, and Nanotechnology*, San Diego CA, 3-5 March 2003, Volume 5055, pages 319-327, ISSN 0277-786X
- <sup>7</sup> Arms, S.W., Hamel, M.J., Townsend, C.P., "Multi-channel Structural Health Monitoring Network, Powered & Interrogated Using Electromagnetic Fields", *Proceedings Society for Advanced Materials Process Engineering (SAMPE)*, Baltimore, MD, 6<sup>th</sup> June 2007